Fingerprinting of Underivatized Monosaccharide Stereoisomers Using High-Resolution Ion Mobility Spectrometry and Its Implications for Carbohydrate Sequencing

Simon Ollivier, Mathieu Fanuel, David Ropartz, Hélène Rogniaux

Fingerprinting of underivatized monosaccharide stereoisomers using high-resolution ion mobility spectrometry and its implications for carbohydrate sequencing

Simon Ollivier,[1,2] David Ropartz,[1,2] Mathieu Fanuel[1,2] and Hélène Rogniaux[1,2]*

[1] INRAE, UR BIA, F-44316 Nantes, France

[2] INRAE, PROBE research infrastructure, BIBS facility, F-44316 Nantes, France

ABSTRACT: Although carbohydrates are the most abundant biopolymers on Earth, there is currently no streamlined method to elucidate their complete sequence. Mass spectrometry (MS) alone is blind to many cases of isomerism, and thus gives incomplete information for carbohydrates. Notably, the coexistence of numerous stereoisomeric monosaccharide subunits is of special concern. Over the last ten years, the coupling of ion mobility spectrometry (IMS) with MS has kept gaining momentum—especially with the advent of high resolution (HR) IMS devices such as cyclic IMS (cIMS). In fact, IMS is sensitive to the gas-phase conformations of molecules and thus, to stereoisomerisms. In this article, we present innovative ion mobility methods on a cIMS instrument that allowed us to build a database of HR-IMS fingerprints for various underivatized monosaccharide stereoisomers. The conditions were fully compatible with MS/MS fragmentation approaches. We further verify that these fingerprints afford the identification of monosaccharidic fragments released upon collisional fragmentation of oligosaccharides. Overall, these results pave the way towards direct sequencing of carbohydrates at the monosaccharide level using HR-IMS.

INTRODUCTION

Carbohydrates are the most abundant biopolymers on Earth: they are ubiquitous among living organisms and are found among animals, plants, algae, fungi and microorganisms alike. Oligosaccharides are notably defined by their number of composing subunits (degree of polymerization DP), by the nature of these subunits and by their connectivity. Obtaining the three levels of information is not amenable today with a single method and requires a time-consuming combination of multiple analytical techniques.[1] Mass spectrometry (MS) offers a solution to directly characterize oligosaccharides, notably thanks to MS/MS fragmentation approaches such as collision-induced dissociation (CID). However, MS and MS/MS are intrinsically blind to (stereo)isomerism—which is a major problem because the monosaccharidic subunits that compose oligo- and polysaccharides are often diastereoisomers or even epimers. Considering that the stereoisomerism and sequence of the composing subunits have a major impact on the properties of oligo- and polysaccharides, this is a key limitation in using MS to study the structure-activity relationship of carbohydrates. However, MS can be combined with other gas-phase methods such as ion mobility spectrometry (IMS) that is sensitive to (stereo)isomerism. Briefly, IMS measures the mobility of ions under the effect of an electric field and a buffer gas, which will in part depend on their conformation (for a review, see Gabelica *et al.*[2]). Since the advent of high-resolution IMS (HR-IMS) setups, the technique has become a highly popular tool for the study of carbohydrates.[3] HR-IMS setups notably include the Select Series Cyclic IMS instrument (cIMS), in which ion mobility measurement is performed by traveling waves of potential (TWIMS) propagating through a cyclic ion mobility cell. This setup affords extended distances for ion mobility measurements and therefore increased resolution. The cIMS instrument, which was used in the present study, is also the only commercial instrument with multi-stage IMS (IMS^n) capabilities.[4]

The hypothesis underlying the present study is that the mobility profile (otherwise called arrival time distribution or ATD) provides, when combined with MS, a signature of the structure and identity of the ion that can be used for sequencing purposes, particularly at high resolving power. Studies by our group and others have shown promising results where comparing oligosaccharidic fragments to reference IMS profiles of oligosaccharides of DP $\geq$ 2 gave access to the complete sequence of larger oligosaccharides.[5,6] Our group notably demonstrated that the same fragments, when released from a tri- or tetrasaccharide, retained the exact same mobility profile.[6] More recently, we further demonstrated that it was generally possible to identify oligosaccharidic fragments by comparison with matching reference IMS profiles even for reputedly unstable structures like furanosides—with the exception of one very specific case where we observed an isomerization of the fragments. However, we proved that the isomerization in that specific case occurred during the fragmentation stage (but independently from the collision energy), and not during the drift of the ion in the IMS stage.[7] Overall, our previous results indicate that mobility profiles of oligosaccharidic fragments are robust enough to envision a

sequencing strategy based on those profiles. However, there exists a wide diversity of structures for oligosaccharides, even for disaccharides. It therefore appears difficult to consider the above approach as a realistic option since it would require (i) relevant purified standards for each unknown structure, which is far from being possible; and (ii) a significant amount of work to assemble an *ad hoc* database from these standards, if they were available.

On the other hand, a sequencing strategy based on a monosaccharide database seems less tedious and attainable. In this strategy, monosaccharides would be sequentially released from the oligosaccharide directly in the gas phase, thereby keeping the information of their sequence in the polymers.

A first important prerequisite is that *specific IMS signatures must be established for each monosaccharide*. Previous attempts have been made at generating fingerprints of monosaccharides using cIMS.[8,9] The two studies established fingerprints of hexoses isomers using multi-pass IMS. In both cases, adduction of a chemical group was used as a mean to increase the mass of monosaccharides up to several times, making it easier to obtain specific IMS profiles. However, a second important prerequisite is that *the monosaccharides' signatures must be comparable with the fragments obtained by CID*. Adduction approaches therefore appear less suitable for our purposes, essentially because covalent derivatization could impact different OH groups on oligosaccharides compared to monosaccharides because of the pre-existing glycosidic bonds—thus precluding the correspondence between the fragments and the library of monosaccharides.

The present work therefore focused on underivatized monosaccharides. It aimed at providing IMS separation conditions to generate specific fingerprints for some of the most common monosaccharides composing plant or bacterial polysaccharides. The study questioned whether these fingerprints can be used to identify monosaccharidic fragments detached from larger oligosaccharides by CID.

EXPERIMENTAL SECTION

Chemicals. The study was performed using pure monosaccharide and oligosaccharide.

Monosaccharides (analytical grade, purity > 98%): D-galactose (Gal), D-glucose (Glc), D-mannose (Man), L-arabinose (Ara), L-ribose (Rib), D-xylose (Xyl), L-fucose (Fuc), D-galacturonic acid (GalA), D-glucuronic acid (GlcA), *N*-acetyl-D-galactosamine (GalNAc), *N*-acetyl-D-glucosamine (GlcNAc) and *N*-acetyl-D-mannosamine (ManNAc) were purchased from Sigma-Aldrich (Saint Quentin Fallavier, France). L-rhamnose (Rha) was purchased from Alfa Aesar (Kandel, Germany).

Oligosaccharides: Maltopentaose (α1,4-glucan), cellopentaose (β1,4-glucan), laminaripentaose (β1,3-glucan), linear mannopentaose (β1,4-mannan), and xylohexaose (β1,4-xylan) were purchased from Megazyme (Wicklow, Ireland). Dextran 1000 (α1,6-glucan in mixture) was purchased from Sigma-Aldrich (Saint Quentin Fallavier, France). Branched mannopentaose (α1,6-mannan branched in α1,3) was purchased from Dextra Laboratories (Reading, UK). Galactopentaose (β1,4-galactan) was kindly provided by Dr Estelle Bonnin (INRAE, UR BIA, F-44316 Nantes, France).

HPLC grade methanol was purchased from Carlo-Erba (Val de Reuil, France). Ultrapure water was produced using a Milli-Q system (Millipore, Burlington, MA, USA). Lithium chloride (LiCl) was purchased from Sigma-Aldrich (Saint Quentin Fallavier, France).

IMS-MS analyses. Pure samples were infused at a concentration of 1µg/mL in 50:50 water/methanol on a SELECT SERIES Cyclic IMS instrument (Waters, Wilmslow, UK), using a syringe pump set to a flow rate of 5 µL/min. Lithium adducts were generated by doping the solvents with 0.1 mM of LiCl, except in the case of hexoses for which 0.01 mM LiCl was used. Ionization in the Z-spray ESI source was performed with the following parameters: capillary voltage 3.0 kV, cone voltage 60 V, source temperature 100 °C, desolvation gas temperature 300 °C, nebulizer pressure 6 Bars. Details about the voltages and pressures applied in the other parts of the mass spectrometer are available in **Supplementary text 1**. The optimized traveling wave parameters for the separation of monosaccharides were: (i) for classical separations, a TW wave height (WH) of 16 V at a wave velocity (WV) of 350 m/s, (ii) for TW ramps an initial WH of 10 V with an increament of 0.2 V/ms up to a maximum of 22 V, still at a WV of 350 m/s. Oligosaccharides were fragmented to give monosaccharidic fragments under IMS/IMS conditions—which we expect to be necessary for sequencing carbohydrates with cIMS—using the protocol fully described in reference [10]. Briefly, a first step of IMS separation was performed on the parent oligosaccharide at a static WH of 16 V and WV of 350 m/s, then they were ejected to a pre-array store cell and collisionally fragmented upon reinjection in the IMS cell, and finally analyzed with the sequences described below. The collision energy was optimized for each oligosaccharide to maximize the release of monosaccharidic fragments.

MS and IMS-MS spectra were recorded on the cIMS instrument using the Quartz software (Waters Embedded Analyzer release 6, Waters, Wilmslow, UK). Data were processed using MassLynx 4.2 and Driftscope 2.9 (both from Waters, Wilmslow, UK). *Importantly, when comparing the IMS profiles of monosaccharidic fragments to the corresponding monosaccharides, the arrival times (t_A) were corrected to give drift times (t_d), which correspond to the effective separation time*. This is done by subtracting the duration of all cIMS events preceding the final separation from the measured t_A. ATDs were smoothed using the Savitzky-Golay algorithm (window size (scan) ± 1, number of smooths: 2).

RESULTS AND DISCUSSION

Designing IMS strategies for monosaccharide fingerprinting

The first step in designing sequences to separate monosaccharides was to optimize the traveling wave parameters. The context of the present study implied that a compromise had to be reached between optimal separation of the monosaccharides and retaining the ability to separate larger oligosaccharides for sequencing purposes. Key TW parameters notably include the wave velocity (WV) and

wave height (WH). We chose to keep the WV at 350 m/s, which is efficient for small and medium-sized ions (*i.e.*, mono- and oligosaccharides). The main parameter we played with to optimize the separation was thus the WH.

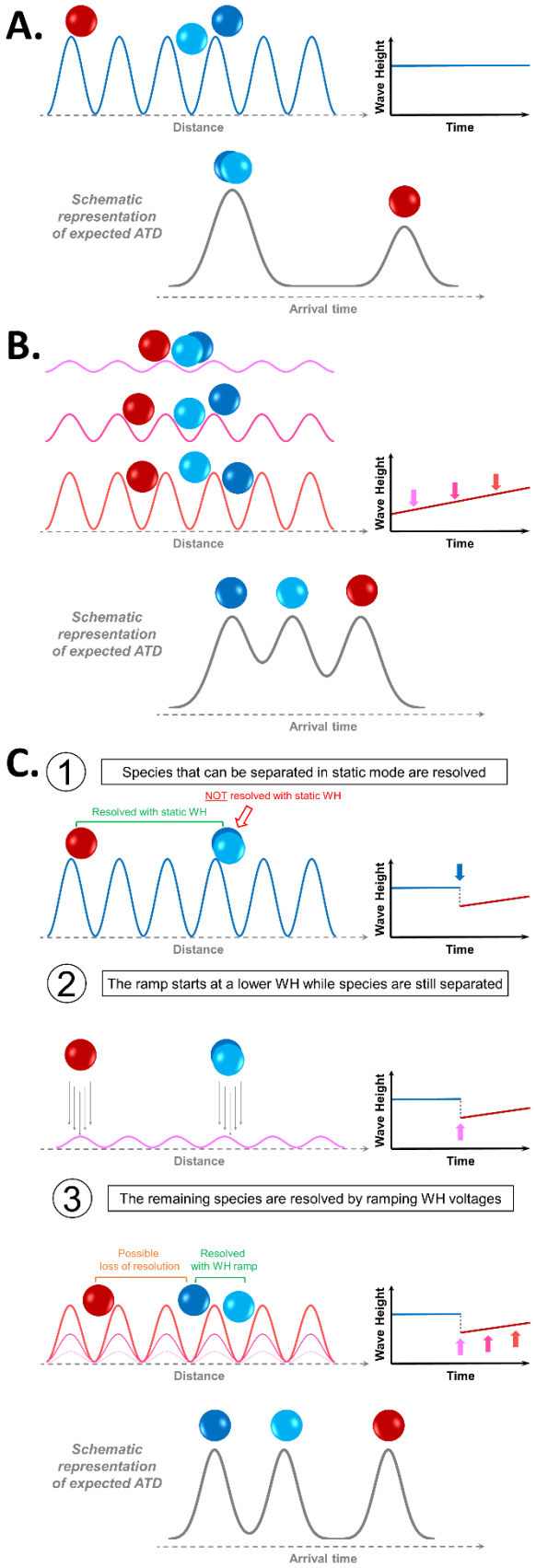

Figure 1. Simplified representations of the TWIMS strategies used in this work (ion clouds and traveling waves not to scale). **A.** Static traveling wave separation. The WH remains constant over time. **B.** Separation with a ramping of the traveling wave height. Different WH are applied over time. **C.** Schematic of the strategy combining static and ramping wave height separations to resolve additional populations

The cIMS setup offers two functionalities to set up the WH in the mobility cell (see more details in **Supplementary text 2**). The first is the static WH functionality, in which a single optimized WH voltage is applied and the WH is kept constant during the entire IMS separation (**Figure 1A**). The second is to ramp the traveling wave height during the IMS separation (**Figure 1B**). Ramping the WH voltages gives more chance that an efficient WH value is reached for the different species at some point, affording the separation of species indistinguishable with a static WH. This mode, however, has the disadvantage that the change in TW parameters over time can result in slightly asymmetrical peaks which, among other processing difficulties, cannot be fitted with Gaussians, a relatively popular strategy for processing ATDs.[11]

In a preliminary test conducted on hexoses, we evaluated the above two strategies using single-pass and multi-pass approaches. To evaluate the capacity to reach specific IMS profiles, we chose as the criterion that peak-picking algorithms must be able to distinguish at least one specific peak for each isomer. As gaussian fitting is not suited to separation with ramping WH, we used the peak detection feature of Driftscope, which accounts for peak tailing. In the case of hexoses, the results obtained using either static or ramping traveling wave were not satisfactory (data not shown). We thus endeavored to develop a method that could give better-resolved profiles for hexoses.

The novel method, described in **Figure 1C**, is a combination of the static and ramping WH sequences. A first step of separation with a static WH is applied until the best separation is obtained on the peaks that can be separated (red vs blue). This is a crucial step because the following step with ramping WH is likely to lower that initial separation. However, it is important not to use an excessive separation here so that ions do not wrap-around during the ramping passes. After the first static WH separation, the WH is lowered to a level at which the unseparated ions (light vs dark blue) are not surfing at the wave velocity (i.e., both at the same velocity) anymore. A WH ramp is then used to gradually get to WH levels where the blue ions are efficiently separated. At the end, this gives an ATD in which all species are resolved, with (i) the blue populations being separated thanks to the WH ramp and (ii) the blue and red populations being separated with a slightly worse—but still satisfactory—resolution compared to static WH strategies.

On a cIMS platform, the combined strategy for WH translates to using two consecutive separation events in the control sequence (the first with a static WH, the second with a ramping WH), the switch ideally being placed right after the ions finish their last "static" pass. Of note, since the ramping WH starts at a lower value compared to the static WH, the "ramping" passes will initially be much slower than the "static" passes. For instance, in the sequence used to obtain the data shown in this article, the

first four "static" passes take *ca*. 20 ms, and the final two "ramping" passes also take *ca*. 20 ms (see the detailed sequences used to separate the monosaccharides in **Table S1**).

Presentation of the samples and choice of the counter-ion

We acquired IMS fingerprints for a series of 13 monosaccharides representative of those composing unmodified plant or bacterial polysaccharides (**Figure 2A**). This consists of 3 hexoses, 3 pentoses, 2 deoxyhexoses, 2 hexuronic acids and 3 *N*-acetyl hexosamines.

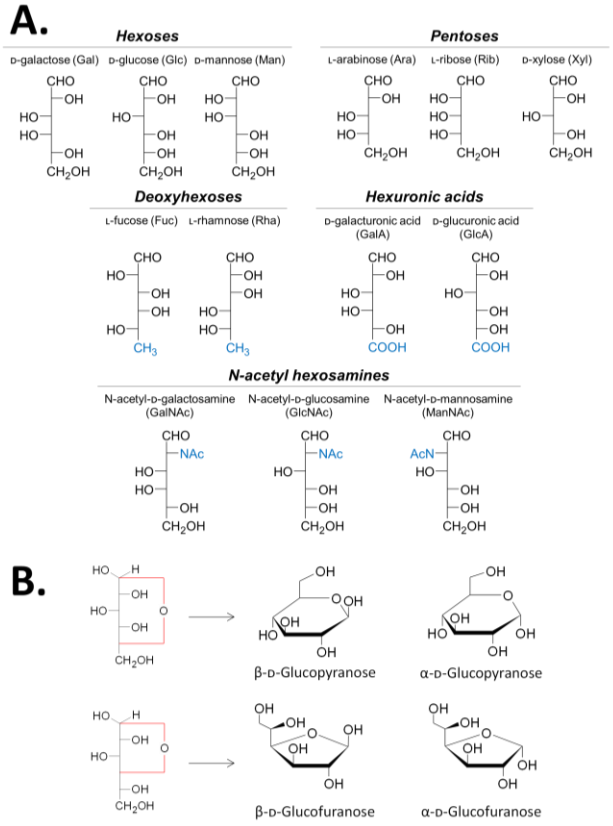

Figure 2. A. Fischer representation of the 13 studied monosaccharides, sorted by isomeric family; **B.** Illustration on D-glucose of the co-existing α/β and pyranose/furanose forms.

Figure 2A presents the monosaccharides using the Fischer representation, but in Nature, different forms of each monosaccharide exist in equilibrium: the α- and β-pyranoses, the α- and β-furanoses (as illustrated for glucose in **Figure 2B**), the pyranose forms typically representing > 90% of the existing species. Therefore, we did not try to achieve baseline separation of the isomers but rather *to obtain distinctive fingerprints for each monosaccharide*.

It is well documented that using different metal counter-ions yields distinctive ATDs, related to the size of the counter ion.[12–14] However, considering our aim of using these fingerprints for sequencing purposes, we also determined which of Li^+ and Na^+ counter ions yielded the highest proportion of detached monosaccharide upon fragmentation.

CID experiments on a glucose homo-oligomer (cellopentaose, **Figure S1**) showed that Li^+ adducts yielded more monosaccharidic fragment compared to Na^+ adducts (which released practically no monosaccharide). We thus opted to work on lithium adducts in the following experiments.

Oligosaccharides can generate isomeric fragments by cleavage of the glycosidic bond (nomenclature according to Domon and Costello,[15] **Figure S2**). These fragments can theoretically correspond to intact mono-/oligosaccharides (Y and C ions, respectively at the reducing and non reducing end), or to dehydrated mono-/oligosaccharides (Z and B ions, respectively at the reducing and non reducing end). In practice, it has been demonstrated on multiple occasions (with ^{18}O-labeling of the reducing end of oligosaccharides) that collisional dissociation of alkali-cationized neutral oligosaccharides yields almost exclusively B and Y ions using Nitrogen as collision gas for CID in the cIMS instrument.[6,16] Herein, for simplicity, we have thus annotated "intact" fragments as Y-type, and dehydrated fragments as B-type.

Fingerprinting of lithiated monosaccharide stereoisomers

Hexose monosaccharides. We established the IMS profiles of glucose (Glc), mannose (Man) and galactose (Gal) using a 4-pass static WH separation, followed by a further 2-pass separation with a ramping WH (**Figure 3A**). It is noteworthy that Man and Gal are both epimers of Glc, in respectively C-2 and C-4.

All three species presented specific bimodal distributions: t_A = 50.2 and 53.1 ms for Glc, t_A = 49.6 and 52.9 ms for Man, and t_A = 49.3 and 50.8 ms for Gal. In an equimolar mixture of the three monosaccharides (black trace), the peak-picking algorithm of Driftscope distinguished the specific features at 49.6, 50.2 and 50.8 ms (inset), and an undistinctive feature at 53 ms (shared between Glc and Man).

In summary, the IMS sequence that we developed yielded at least one distinctive peak for each hexose monosaccharide.

Pentose monosaccharides. We recorded the fingerprints for arabinose (Ara), xylose (Xyl) and ribose (Rib) using a 4-pass ramping separation (**Figure 3B,** top). Ara and Rib are epimers in C-2.

Contrary to hexoses, we did not observe a systematic bimodal distribution. Rib exhibited a single peak at 36.3 ms, Xyl exhibited a bimodal distribution at 36.2 and 37.1 ms, and Ara exhibited a multimodal pattern with peaks at 37.1 and 39.4 ms and a shoulder around 36.5 ms.

Because of ionization competition, we analyzed non-equimolar mixtures of the monosaccharides with a significantly higher concentration of Ara. In the mixture, the Driftscope peak-picking algorithm detected features at 36.2, 37.1 and 39.4 ms. Only the feature at 39.4 ms is distinctive of Ara, the feature at 36.3 ms being shared between Rib and Xyl and that at 37.1 ms between Ara and Xyl.

However, Rib is rarely found in polysaccharides in conjunction with Ara and Xyl and plant polysaccharides almost exclusively contain Ara and Xyl. When considering a mixture containing only Ara and Xyl (**Figure 3B**, bottom), the peak detection algorithm points one peak which is specific for Xyl (at 36.2 ms), and one peak which is specific of Ara (at 39.4 ms). We thus considered that the separation

conditions were satisfactory for our purposes, as they allow to clearly distinguish Ara and Xyl.

Deoxyhexose (a.k.a. methylpentose) monosaccharides. We recorded fingerprints for fucose (Fuc) and rhamnose (Rha) using a 4-pass ramping separation (**Figure 3C**).

Both exhibited multimodal ATDs, with two major peaks each (for Fuc, t_A = 37.8 and 38.6 ms and for Rha, t_A = 39.6 and 41.9 ms). In an equimolar mixture of Fuc and Rha, the Driftscope peak picking easily detected features at 37.8, 38.6, 39.6, and 41.9 ms corresponding to the four major features of the two monosaccharides.

Hexuronic acid monosaccharides (HexA). Hexuronic acid are derivatives of hexoses in which the hydroxymethyl group in C-5 is oxidized, giving a carboxyl group. Fingerprints were obtained for glucuronic acid (GlcA) and galacturonic acid (GalA) using a 4-pass ramping separation (**Figure 3D**). GlcA and GalA are epimers in C-4.

Both ATDs exhibited multimodal distributions with two major features (for GalA, t_A = 39.6 and 41.2 ms and for GlcA t_A = 40.2 and 43.0 ms). In an equimolar mixture of GalA and GlcA, the Driftscope peak picking was able to detect the feature at 41.2 ms for GalA, and both features at 40.2 and 43.0 ms for GlcA.

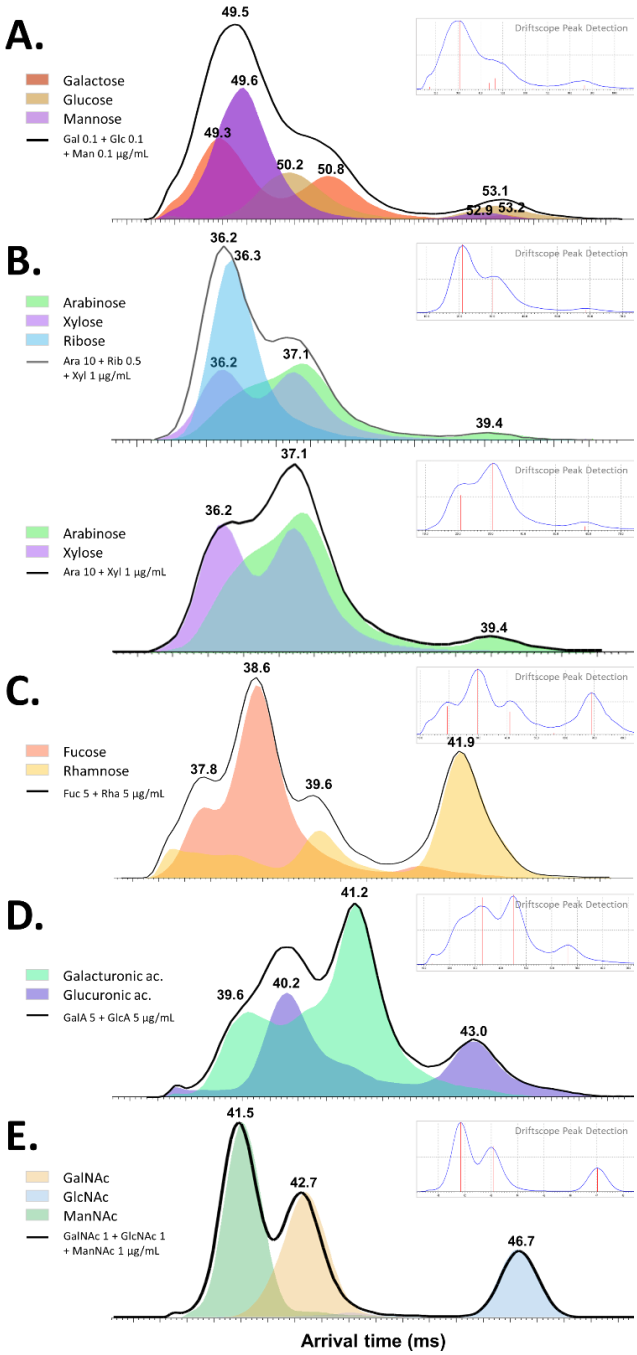

Figure 3. Arrival time distributions for the monosaccharides (colored), including **A.** Hexoses (isolated as $[M+Li]^+$ *m/z* 187.1); **B.** Pentoses ($[M+Li]^+$ *m/z* 157.1); **C.** Deoxyhexoses ($[M+Li]^+$ *m/z* 171.1); **D.** Hexuronic acids ($[M+Li]^+$ *m/z* 201.1) and **E.** *N*-acetyl hexosamines ($[M+Li]^+$ *m/z* 228.1), and arrival time distributions for mixtures of each isomeric family (solid lines). Insets: results of the Driftscope peak detection of the mixtures.

N-Acetyl hexosamine monosaccharides (HexNAc). HexNAc are hexoses derivatives, for which the hydroxyl group in C-2 is replaced by an *N*-acetylation, they are common in bacterial polysaccharides. We recorded IMS fingerprints for *N*-acetyl glucosamine (GlcNAc), *N*-acetyl mannosamine (ManNAc) and *N*-acetyl galactosamine (GalNAc) using a 5-pass static WH separation (**Figure 3E**). ManNAc and GalNAc are epimers of GlcNAc in C-2 and C-4, respectively.

Interestingly, contrary to what we observed on all previous types of reducing monosaccharides (*i.e.*, subject to the mutarotation phenomenon thus to the α/β and pyranose/furanose equilibriums), the HexNAc monosaccharides only exhibited one major peak each, at t_A = 46.7 ms for GlcNAc, 42.7 ms for ManNAc, and 41.5 ms for ManNAc. One hypothesis could be the existence of an ultra-preferential coordination of the Li^+ cation involving the *N*-acetyl group, resulting in the observation of a single conformer.

All three species were relatively well resolved, and GlcNAc was notably baseline-resolved from GalNAc and ManNAc. They were thus readily distinguished in an equimolar mixture.

In this section, using different types of TWIMS functionalities on a cIMS platform, including innovative sequences that combined static and ramping traveling waves, we were able to establish specific signatures for five isomeric families of monosaccharides, among the most common in plant and bacterial polysaccharides. Importantly, these signatures were obtained for underivatized monosaccharides in relatively short IMS analysis times (all between 20 and 40 ms, see **Table S1**).

Of note, while multimodal distribution of alkali-cationized oligosaccharides have been previously linked to separation of α/β anomers,[14] it seems unlikely here that different peaks arise from different anomers. Indeed, if all studied monosaccharides were reducing saccharides, their observed IMS profiles did not match in general the reported mutarotation equilibrium. For instance, ribose only presented one major peak whereas the reported abundances of its different forms are: α-ribopyranose 21,5%, β-ribopyranose 58.5%, α-ribofuranose 6,5%, and β-ribofuranose 13.5%.[17] This hints towards the observed profiles being more likely related to conformers—although a link between conformation and anomerism cannot be fully excluded.

The strategies that we developed in this study can be extended to other types of adducts than $[M + Li]^+$. For instance, IMS profiles obtained on $[M + Na]^+$ adducts of hexoses and hexuronic acids are shown in **Figures S3-4**.

We further showed that signature peaks could be identified in the ATDs by processing software even in mixtures of stereoisomeric monosaccharides, which might prove useful to deconvolve data generated in sequencing approaches (likely to contain the signatures of multiple monosaccharides).

Monosaccharidic fragments from homo-oligosaccharides match the profile of monosaccharides

One key step in the envisioned sequencing strategy is to validate that the monosaccharidic fragments generated by CID from larger oligosaccharides match the drift time of the monosaccharidic references. We performed this verification with homo-oligomers (DP5 or DP6) of hexoses and pentoses, which are the easiest to procure.

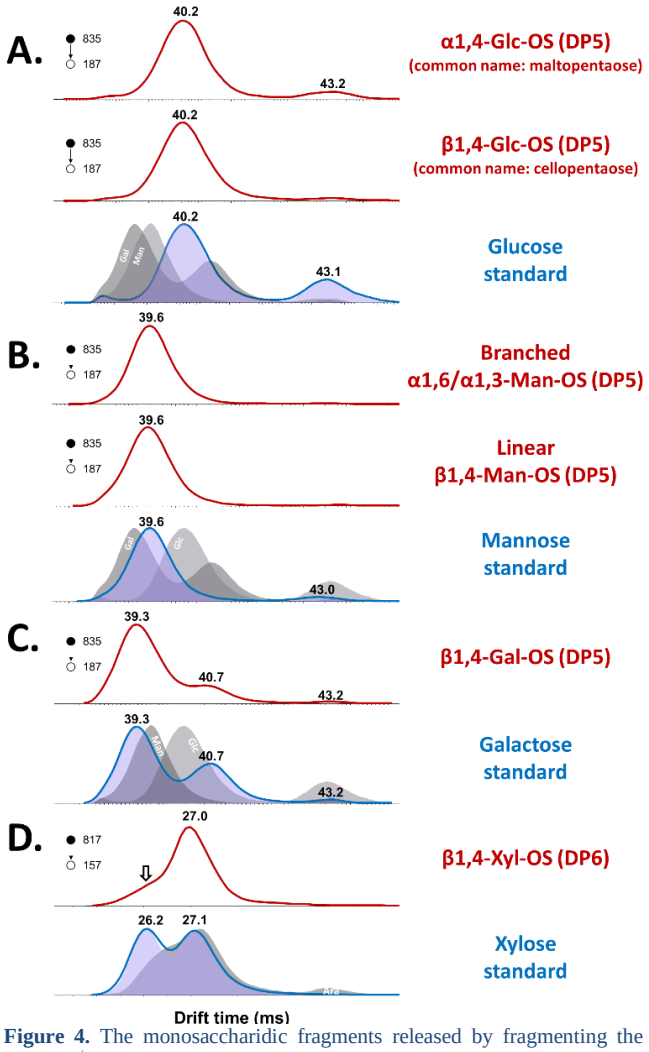

Figure 4. The monosaccharidic fragments released by fragmenting the $[M + Li]^+$ species of various oligohexoses (**A.** Glc-OS, **B.** Man-OS and **C.** Gal-OS) and oligopentose (**D.** Xyl-OS) in red, are compared to the reference profiles of the corresponding monosaccharides in blue, and reference profiles of other monosaccharides from the same family in grey.

Gluco-oligosaccharides (Glc-OS). Two structures were studied: α1,4- and β1,4-Glc-OS DP5. As shown in **Figure 4A**, the monosaccharidic fragments (Glc_1 at $[M + Li]^+$ *m/z* 187.1) produced from both were a good match to the IMS profile of pure glucose. Notably, the major Glc peak at a drift time t_d = 40.2 ms remained the main feature of the IMS profile of the fragments. Of note, the feature at 43.1 ms was observed with less intensity on the fragments compared to pure Glc, but this peak was more intense for maltopentaose (α1,4-Glc-OS DP5) compared to cellopentaose (β1,4-Glc-OS DP5). In a previous work, we established that, upon IMS^n experiments, the anomerism of the internal bond was retained within DP2 fragments in mannosides.[6] What is observed here rather suggests an *imprint of the anomerism left by the cleaved glycosidic bond on the IMS profile after its dissociation*. Such "anomeric memory" in monosaccharidic fragments has been established before using MS coupled to gas-phase infrared spectroscopy,[18,19] as well as by low-resolution (LR)-IMS after CID by Gray et al.[20] This will be studied in more detail in the later parts of this article.

Manno-oligosaccharides (Man-OS). We likewise observed that the monosaccharidic fragments released at *m/z* 187.1 (Man_1 as $[M + Li]^+$ species) from two different Man-OS of DP5 were a good match to the profile of pure Man (**Figure 4B**). The IMS profiles unambiguously exhibited a major feature at 39.6 ms, which was the signature peak of Man. Of note, the Man feature at 43.0 ms was not observed for the OSs.

Galacto-oligosaccharides (Gal-OS). One β1,4-Gal-OS of DP5 was studied (**Figure 4C**). The profile of its monosaccharidic fragment (Gal_1, detected at *m/z* 187.1 as $[M + Li]^+$) was a near-perfect match to that of pure Gal. Indeed, we detected all three peaks of Gal at t_d = 39.3, 40.7, and 43.2 ms, respectively (albeit a slightly lower intensity for the 40.7 ms feature in the fragment compared to the reference).

Xylo-oligosaccharides (Xyl-OS). Finally, we measured the IMS profiles of fragments for one Xyl-OS of DP6 (**Figure 4D**). Its monosaccharidic fragment (Xyl_1, detected as $[M + Li]^+$ at *m/z* 157.1) matched the profile of the reference Xyl. We note that the main peak in the fragment's IMS profile is t_d = 27.0 ms, which is also close to a peak found in the profile of Ara (grey trace and **Figure 3B**). Nevertheless, the feature at 26.2 ms is also observed in the form of a shoulder of significant intensity, and the start/end times of the drift time distribution are identical to the standard.

Overall, in all evaluated cases of homo-oligomers (hexoses and pentoses, DP5 and DP6), the IMS profile of the monosaccharidic fragments released by CID matched the IMS profile of the corresponding monosaccharides, which supports the relevance of the approach to a sequencing strategy. In addition, a potential signature of the anomericity of the broken glycosidic bond was observed on the IMS profile, notably in the case of glucosides. Importantly, the above-mentioned study by Gray et al. already demonstrated a match between glycosidic fragments and reference LR-IMS profiles of different monosaccharides. However, their IMS profiling conditions did not afford the discrimination of monosaccharide stereoisomers and had to be combined with offline IR spectroscopy. In the present work, by combining this strategy with the specificity of our newly obtained HR-IMS fingerprints, we demonstrate that *it is now possible to directly identify the detached monosaccharide with IMS*, even for diastereoisomeric and epimeric subunits.

Does the HR-IMS profile of the monosaccharidic fragments reflect the anomerism (or regioisomerism) of the linkage in the parent oligosaccharide?

The above question was addressed through the study of various types of Glc-OS. Indeed, glucosides are abundant and ubiquitous in Nature and offer a wide variety of linkage isomers, most of them being available as commercial standards of good purity. In **Figure 5**, we present the IMS profiles for four Glc-OS of DP5: two α-linked Glc-OS (dextran and maltopentaose, linked in α1,6 and α1,4 respectively), and two β-linked Glc-OS (cellopentaose and laminarin, linked in β1,4 and β1,3 respectively). In all cases, the main peak in the IMS profile of the monosaccharidic fragment at *m/z* 187.1 was that at 40.2 ms. However, for the two α-linked glucans, the feature at 43 ms was more intense compared to the two β-linked glucans.

The two features at 40.2 and 43.1 ms cannot, however, be directly correlated to the α or β anomers as we observe the 40.2 ms feature in both α and β-linked Glc-OS and a slight trace of the 43 ms feature in the profile of one of the two β-linked Glc-OS studied (the cellopentaose). Still, it appears that some features of the ATD are influenced by the anomeric configuration of the linkage, which is an interesting property, as it could help assign the intrachain anomerism during the sequencing of oligosaccharides. A possible explanation for this difference between the IMS fingerprints of α- and β-anomers would be the existence of preferential coordination of the Li^+ cation depending on the stereochemistry of the anomeric carbon (i.e., of the glycosidic bond).

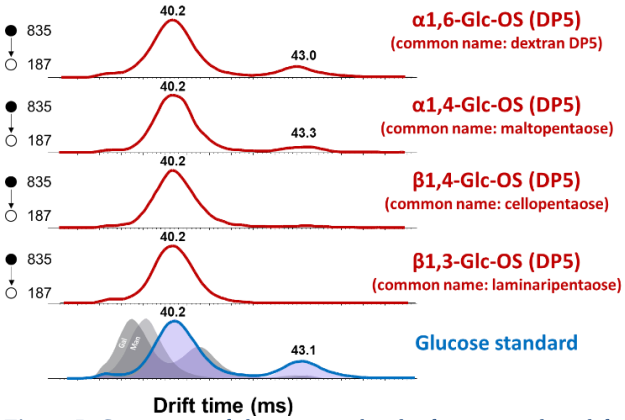

Figure 5. Comparison of the monosaccharidic fragments released from different gluco-oligosaccharides isolated at *m/z* 835.3 as $[M + Li]^+$ with α (DP5 dextran in α1,6 and maltopentaose in α1,4) or β linkages (cellopentaose in β1,4 and laminaripentaose in β1,3). In blue, the IMS profile of pure glucose is given for reference.

Can we work on B-type fragment ions?

In all of the above results, the Y_1 ion was considered in the fragmentation spectra. However, sequencing carbohydrates in both directions (i.e., from the reducing end to the non-reducing end and vice versa) would increase confidence in structural assignments. Furthermore, the ratio between B and Y fragments intensities can vary depending on the oligosaccharides (e.g., **Figure S5**) and it would sometimes be easier to sequence oligosaccharides using the B ion series. We thus aimed at determining if the sequencing strategy could be envisaged from B ions, since B_1 ions correspond to a dehydrated equivalent of the reference monosaccharides.

Impact of the glycosidic bond (regioisomerism and anomerism) on the IMS profile of B_1 fragments. **Figure 6A** presents the HR-IMS profiles of the dehydrated monosaccharidic fragments (*m/z* 169.1) of the four Glc-OSs of DP5 after three IMS passes, which we consider to be B_1 fragments. Despite a few intensity differences for some features, we observed very similar profiles between the two α-Glc-OSs on one hand, and the two β-Glc-OSs on the other hand. However, very different profiles were observed between α and β glucans. Indeed, both α-linked species exhibit a multimodal profile containing features at 68.5, 69.4, 71.1, and 72.8 ms, while both β-linked species exhibit a simpler profile with a major peak at 69.3 ms and

minor features at 68.5 and 71.2 ms. This finding is interesting because it suggests that IMS profiles of the dehydrated monosaccharides (B_1 fragments) sign the anomerism of the bond.

Impact of the epimerism of the subunit on the IMS profile of B_1 fragments. It was key to assess whether the IMS signatures of B_1 fragments were unique to the subunit (in the previous case, Glc). Indeed, the dehydration of different stereoisomers (such as Glc and Gal, or Glc and Man) could potentially give the exact same B_1 fragment structure. We thus analyzed three hexosides of DP5 composed either of Glc, Man or Gal subunits, all linked with β1,4 bonds (**Figure 6B**). The dehydrated monosaccharidic B_1 fragment produced by the Gal-OS DP5 exhibited a very distinctive IMS profile composed of many features (at 68.0, 69.6, 70.7 and 71.5 ms). However, the IMS profile of the *m/z* 169.1 fragment produced from the Man-OS DP5 was strikingly similar to that produced from the Glc-OS DP5.

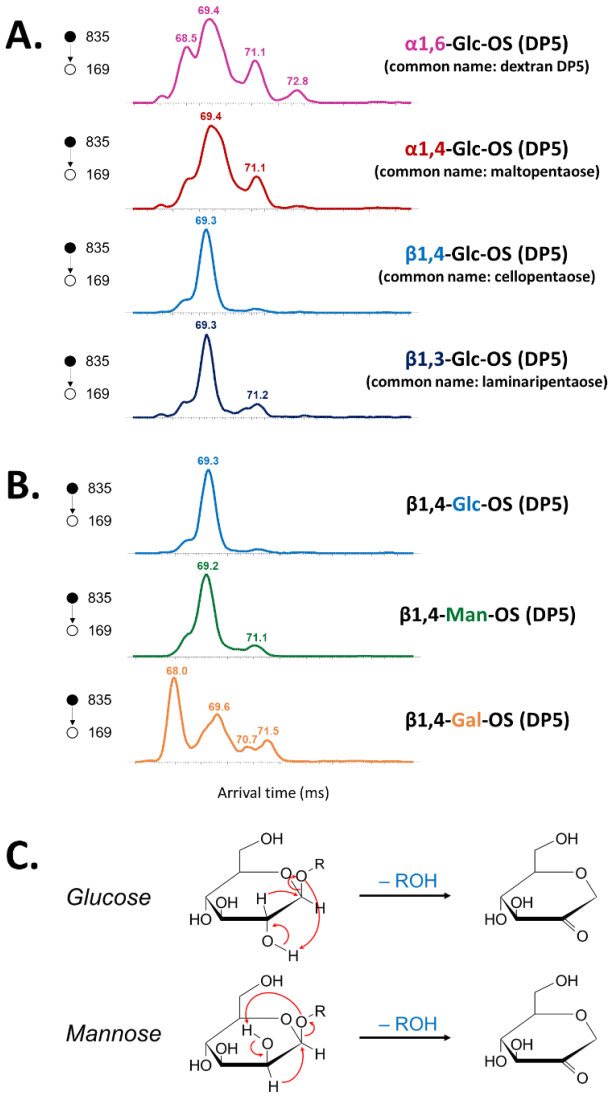

Figure 6. Comparison of the dehydrated monosaccharidic fragments (B_1, *m/z* 169.1 as $[M + Li]^+$ species) released **A.** from different Glc-OS of DP5 with varying α or β linkages; **B.** from β1,4-linked Glc-OS DP5, Man-OS DP5 and Gal-OS DP5. Parent ions were isolated at *m/z* 835.3 (Hex_5 as $[M + Li]^+$). The presented ATDs were acquired after three passes around the IMS cell (static WH conditions). **C.** Fragmenting a Glc-β1,4-Glc or a Man-β1,4-Man bond gives the same B_1 fragment. One of the possible dehydration mechanisms (see Abutokaikah *et al.*[21]) is presented for both Glc and Man subunits (R = oligosaccharidic chain).

To our understanding, this is actually the result of Glc and Man being C-2-epimers. Upon dissociation of the glycosidic bond and dehydration, a double bond can form between C-2 and O-2 (see fragmentation scheme in **Figure 6C**), resulting in the B_1 fragment losing the stereospecificity that would allow to distinguish Glc and Man.

In summary, despite the potential interest of B_1 fragments to sign the intrachain anomerism of the oligosaccharide, using them alone is not an option since they do not allow to discriminate all building blocks occurring in natural polysaccharides. Nevertheless, they could still be an interesting complement to Y_1 fragments for cross validation of the sequence.

CONCLUSION

In this study we have proved that HR-IMS could be used to obtain distinctive fingerprints of underivatized isomeric monosaccharides. These fingerprints can be used to identify monosaccharidic fragments produced by CID of larger oligosaccharides—which forms the basis of a sequencing method of carbohydrates relying on HR-IMS.

We designed innovative ion mobility sequences on a cIMS instrument that afforded the distinction of several monosaccharides from five families of diastereoisomers (hexoses, pentoses, deoxyhexoses, hexuronic acids and *N*-acetyl hexosamines). In agreement with the LR-IMS literature,[20] we confirmed that Y_1 fragments released upon CID of homo-oligosaccharides matched the HR-IMS profiles of monosaccharides, and we also observed that the connectivity of the subunits in the parent oligosaccharide left an imprint on the IM profile of monosaccharidic fragments. We now demonstrate that these properties, combined with our HR-IMS fingerprinting strategy, afford direct identification of the detached monosaccharide. We further showed that B_1 ions (dehydrated monosaccharides) could possibly complement the information obtained from Y_1 fragments, but with the restriction that some epimers could give identical B_1 fragments. Finally, our results suggest that the intrachain anomerism can be inferred from the IMS profiles of the fragments.

Overall, the results presented in this article suggest that cIMS shows great potential for the *de novo* sequencing of carbohydrates, thereby addressing an analytical lock that dates back several years. In the future, it will be interesting to see whether the presented fingerprinting strategy can be extended to other high-resolution IMS setups, such as Trapped IMS (TIMS) or Structures for Lossless Ion Manipulation (SLIM).

ASSOCIATED CONTENT

Supporting Information

Detailed instrument parameters; mobility sequences; Domon and Costello fragmentation nomenclature; example MS/MS spectra; IMS fingerprints for $[M+Na]^+$ species (PDF)

AUTHOR INFORMATION

Corresponding Author

* Hélène Rogniaux (helene.rogniaux@inrae.fr)

Author Contributions

The manuscript was written through contributions of all authors. All authors have given approval to the final version of the manuscript.

Notes

The authors declare no competing financial interest.

ACKNOWLEDGMENT

The authors would like to thank GIS IBiSA, Nantes Métropole, Région Pays de la Loire and FEDER for financial support in purchasing a SELECT SERIES Cyclic IMS instrument. S.O. acknowledges the French National Research Agency for funding of his Ph.D. (grant ANR-18-CE29-0006).

REFERENCES

(1) Gray, C. J.; Migas, L. G.; Barran, P. E.; Pagel, K.; Seeberger, P. H.; Eyers, C. E.; Boons, G.-J.; Pohl, N. L. B.; Compagnon, I.; Widmalm, G.; Flitsch, S. L. Advancing Solutions to the Carbohydrate Sequencing Challenge. *J. Am. Chem. Soc.* **2019**, *141* (37), 14463–14479.

(2) Gabelica, V.; Marklund, E. Fundamentals of Ion Mobility Spectrometry. *Curr. Opin. Chem. Biol.* **2018**, *42*, 51–59.

(3) Delafield, D. G.; Lu, G.; Kaminsky, C. J.; Li, L. High-End Ion Mobility Mass Spectrometry: A Current Review of Analytical Capacity in Omics Applications and Structural Investigations. *TrAC Trends in Analytical Chemistry* **2022**, *157*, 116761.

(4) Giles, K.; Ujma, J.; Wildgoose, J.; Pringle, S.; Richardson, K.; Langridge, D.; Green, M. A Cyclic Ion Mobility-Mass Spectrometry System. *Anal. Chem.* **2019**, *91* (13), 8564–8573.

(5) Miller, R. L.; Guimond, S. E.; Schwörer, R.; Zubkova, O. V.; Tyler, P. C.; Xu, Y.; Liu, J.; Chopra, P.; Boons, G.-J.; Grabarics, M.; Manz, C.; Hofmann, J.; Karlsson, N. G.; Turnbull, J. E.; Struwe, W. B.; Pagel, K. Shotgun Ion Mobility Mass Spectrometry Sequencing of Heparan Sulfate Saccharides. *Nat Commun* **2020**, *11* (1), 1481.

(6) Ollivier, S.; Tarquis, L.; Fanuel, M.; Li, A.; Durand, J.; Laville, E.; Potocki-Veronese, G.; Ropartz, D.; Rogniaux, H. Anomeric Retention of Carbohydrates in Multistage Cyclic Ion Mobility (IMSn): De Novo Structural Elucidation of Enzymatically Produced Mannosides. *Anal. Chem.* **2021**, *93* (15), 6254–6261.

(7) Ollivier, S.; Legentil, L.; Yeni, O.; David, L.-P.; Ferrières, V.; Compagnon, I.; Rogniaux, H.; Ropartz, D. Gas-Phase Behavior of Galactofuranosides upon Collisional Fragmentation: A Multistage High-Resolution Ion Mobility Study. *J. Am. Soc. Mass Spectrom.* **2023**, *34* (4), 627–639.

(8) McKenna, K. R.; Li, L.; Baker, A. G.; Ujma, J.; Krishnamurthy, R.; Liotta, C. L.; Fernández, F. M. Carbohydrate Isomer Resolution via Multi-Site Derivatization Cyclic Ion Mobility-Mass Spectrometry. *Analyst* **2019**, *144* (24), 7220–7226.

(9) Williamson, D. L.; Nagy, G. Evaluating the Utility of Temporal Compression in High-Resolution Traveling Wave-Based Cyclic Ion Mobility Separations. *ACS Meas. Au* **2022**, *2* (4), 361–369.

(10) Ollivier, S.; Fanuel, M.; Rogniaux, H.; Ropartz, D. Using a Cyclic Ion Mobility Spectrometer for Tandem Ion Mobility Experiments. *J. Vis. Exp.* **2022**, *179*, e63451.

(11) Polasky, D. A.; Dixit, S. M.; Fantin, S. M.; Ruotolo, B. T. CIUSuite 2: Next-Generation Software for the Analysis of Gas-Phase Protein Unfolding Data. *Anal. Chem.* **2019**, *91* (4), 3147–3155.

(12) Huang, Y.; Dodds, E. D. Ion Mobility Studies of Carbohydrates as Group I Adducts: Isomer Specific Collisional Cross Section Dependence on Metal Ion Radius. *Anal. Chem.* **2013**, *85* (20), 9728–9735.

(13) Huang, Y.; Dodds, E. D. Discrimination of Isomeric Carbohydrates as the Electron Transfer Products of Group II Cation Adducts by Ion Mobility Spectrometry and Tandem Mass Spectrometry. *Anal. Chem.* **2015**, *87* (11), 5664–5668.

(14) Williamson, D. L.; Bergman, A. E.; Nagy, G. Investigating the Structure of α/β Carbohydrate Linkage Isomers as a Function of Group I Metal Adduction and Degree of Polymerization as Revealed by Cyclic Ion Mobility Separations. *J. Am. Soc. Mass Spectrom.* **2021**, *32* (10), 2573–2582.

(15) Domon, B.; Costello, C. E. A Systematic Nomenclature for Carbohydrate Fragmentations in FAB-MS MS Spectra of Glycoconjugates. *Glycoconjugate J.* **1988**, *5* (4), 397–409.

(16) Ujma, J.; Ropartz, D.; Giles, K.; Richardson, K.; Langridge, D.; Wildgoose, J.; Green, M.; Pringle, S. Cyclic Ion Mobility Mass Spectrometry Distinguishes Anomers and Open-Ring Forms of Pentasaccharides. *J. Am. Soc. Mass Spectrom.* **2019**, *30* (6), 1028–1037.

(17) Collins, P. M. *Dictionary of Carbohydrates*; CRC Press, 2005.

(18) Schindler, B.; Barnes, L.; Renois, G.; Gray, C.; Chambert, S.; Fort, S.; Flitsch, S.; Loison, C.; Allouche, A.-R.; Compagnon, I. Anomeric Memory of the Glycosidic Bond upon Fragmentation and Its Consequences for Carbohydrate Sequencing. *Nat Commun* **2017**, *8* (1), 973.

(19) Pellegrinelli, R. P.; Yue, L.; Carrascosa, E.; Warnke, S.; Ben Faleh, A.; Rizzo, T. R. How General Is Anomeric Retention during Collision-Induced Dissociation of Glycans? *J. Am. Chem. Soc.* **2020**, *142* (13), 5948–5951.

(20) Gray, C. J.; Schindler, B.; Migas, L. G.; Pičmanová, M.; Allouche, A. R.; Green, A. P.; Mandal, S.; Motawia, M. S.; Sánchez-Pérez, R.; Bjarnholt, N.; Møller, B. L.; Rijs, A. M.; Barran, P. E.; Compagnon, I.; Eyers, C. E.; Flitsch, S. L. Bottom-Up Elucidation of Glycosidic Bond Stereochemistry. *Anal. Chem.* **2017**, *89* (8), 4540–4549.

(21) Abutokaikah, M. T.; Frye, J. W.; Tschampel, J.; Rabus, J. M.; Bythell, B. J. Fragmentation Pathways of Lithiated Hexose Monosaccharides. *J. Am. Soc. Mass Spectrom.* **2018**, *29* (8), 1627–1637.

Insert Table of Contents artwork here

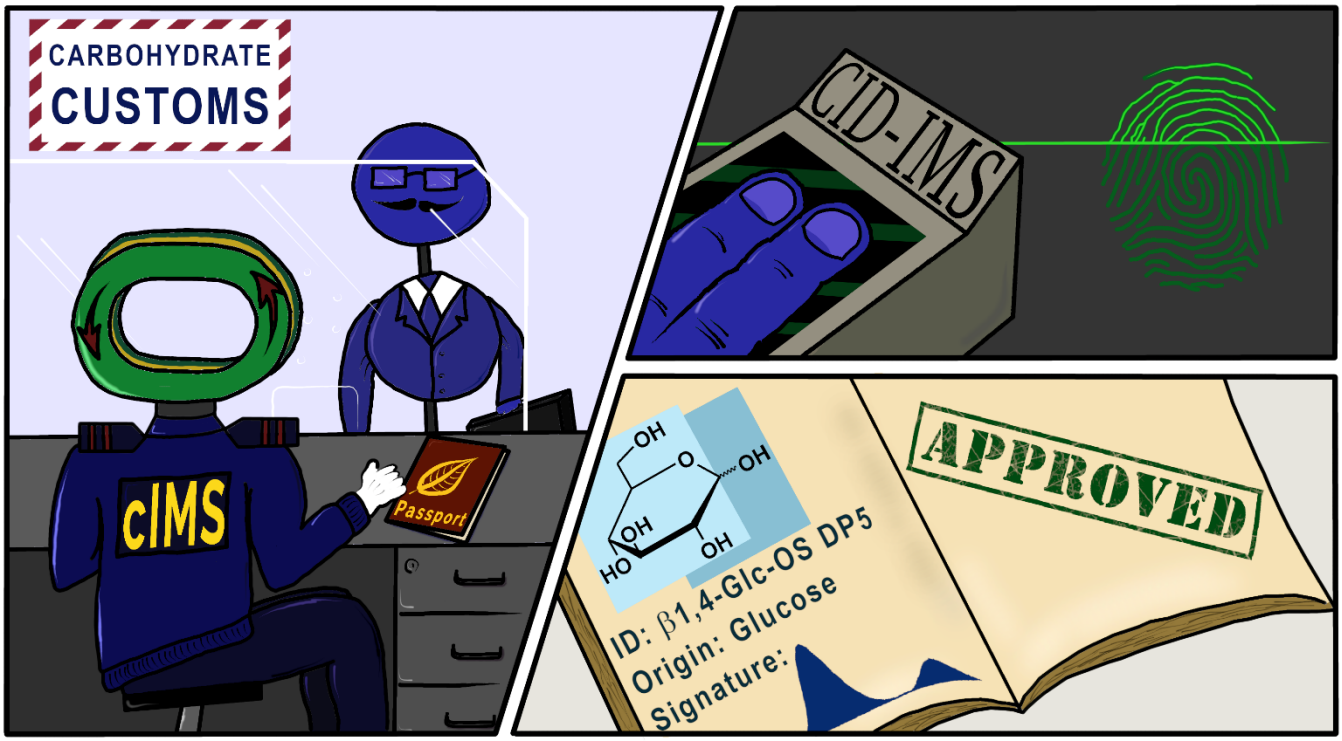
CARBOHYDRATE
CUSTOMS
cIMS
Passport
CID-IMS
APPROVED
OH
O
OH
OH
OH
HO
ID: β1,4-Glc-OS DP5
Origin: Glucose
Signature: